Nuclear Engineering and Technology 55 (2023) 4350–4356

Contents lists available at ScienceDirect

Nuclear Engineering and Technology

journal homepage: www.elsevier.com/locate/net

Original Article

Non-iterative pulse tail extrapolation algorithms for correcting nuclear pulse pile-up

Mohammad-Reza Mohammadian-Behbahani

School of Mechanical Engineering, Shiraz University, Shiraz, Iran

ARTICLE INFO

Keywords:
Non-iterative exponential fitting
Pile-up correction
Pulse tail extrapolation
Radiation detector
Spectroscopy

ABSTRACT

Radiation detection systems working at high count rates suffer from the overlapping of their output electric pulses, known as pulse pile-up phenomenon, resulting in spectrum distortion and degradation of the energy resolution. Pulse tail extrapolation is a pile-up correction method which tries to restore the shifted baseline of a piled-up pulse by extrapolating the overlapped part of its preceding pulse. This needs a mathematical model which is almost always nonlinear, fitted usually by a nonlinear least squares (NLS) technique. NLS is an iterative, potentially time-consuming method.

The main idea of the present study is to replace the NLS technique by an integration-based non-iterative method (NIM) for pulse tail extrapolation by an exponential model. The idea of linear extrapolation, as another non-iterative method, is also investigated. Analysis of experimental data of a NaI(Tl) radiation detector shows that the proposed non-iterative method is able to provide a corrected spectrum quite similar with the NLS method, with a dramatically reduced computation time and complexity of the algorithm. The linear extrapolation approach suffers from a poor energy resolution and throughput rate in comparison with NIM and NLS techniques, but provides the shortest computation time.

1. Introduction

Pulse-mode radiation detection systems are widely used in radiation spectroscopy and imaging. The idea is to have an individual pulse for each single particle which interacts with the detector active volume. To achieve the energy information, the pulse amplitude must be proportional to the amount of the energy the particle transfers to the detector medium. For the case of photon detection, inorganic scintillation detectors (like NaI(Tl)) and semiconductor detectors (most often Si and Ge) are usually used, each one benefiting from some advantages at the expense of some shortcomings [1–3].

Scintillation detectors use a chain of scintillator crystal, photocathode and photomultiplier tube to convert the incident gamma-ray photons to optical photons, optical photons to electrons, and few electrons to a large number of electrons, respectively. The detector output signals are usually read out by a cascade of preamplifier and amplifier (shaper). Scintillation detectors can be made in large sizes with high-atomic-number materials to enhance the detection efficiency. However, their energy resolution is quite poor, mainly due to the photoelectron statistics. Semiconductor detectors, on the other hand, benefit from an excellent energy resolution, usually at the expense of their lower atomic number and detector size [1]. Recently, semiconductor detectors of higher atomic number (like CdTe and CdZnTe) have also been developed for gamma-ray spectroscopy, with improved detection efficiency and room temperature performance near to the cooled Ge detectors [4,5].

Particle emission from radiation sources has a random nature. This means that the start time of the detector pulses is not predictable: some pulses may be far apart in time and some others so close that their pile-up becomes inevitable. When this happens, some newcoming pulses ride on the tail(s) of preceding pulses, therefore their amplitude (energy information) are mismeasured. This effect degrades the energy information of the system by shifting the energy peaks to wrong spectrum channels and by smearing the energy resolution [1,6,7].

So far, there have been proposed several solutions to deal with this problem, from pile-up prevention to rejection and correction methods [8]: in pile-up prevention, the pulses are shortened by analog or digital electronic filtering to avoid pulse overlapping. In rejection strategy, all infectious pulses are discarded. In pile-up correction, we try not to lose information by rejecting pulses, but to recover their true information by numerical procedures.

There exist various pulse information recovery approaches in the literature [9]. Template matching methods assume a fixed pulse

E-mail address: m.mohammadian@saadi.shirazu.ac.ir.

https://doi.org/10.1016/j.net.2023.08.011
Received 8 April 2023; Received in revised form 8 July 2023; Accepted 4 August 2023
Available online 7 August 2023

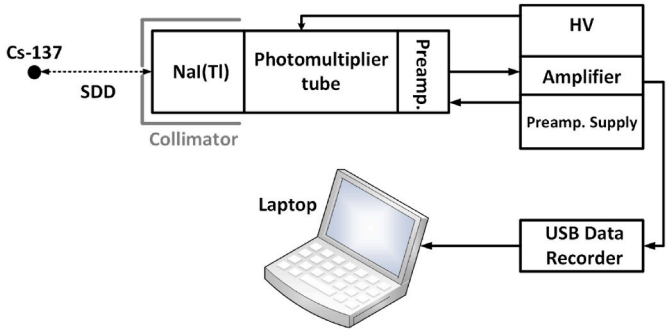

Fig. 1. Radiation detection chain for experimental data acquisition. A ^{137}Cs source is placed at two different source-to-detector distances (SDDs) 80 and 20 cm. NaI(Tl) scintillator is coupled to a preamplifier, amplifier (shaper), and a USB InstruStar-ISDS205A data recorder card. Digitized data are finally saved and analyzed by a laptop computer.

template, a good assumption for the case of scintillation detectors, to establish a transfer matrix that describes the relation between the measured and the true pulse amplitudes [10,11]. High yield pile-up event recover (HYPER) technique [12] characterizes each individual pulse by a single-term exponential decay as:

$$V[n] = A_1 e^{-\alpha_1 n} \quad (1)$$

where V[n] describes the discrete-form voltage signal for which n = 1, 2, 3, …, N, where N is the number of samples in V[n]. A_1 represents the amplitude and α_1 the decay constant of the exponential term. Based on this assumption, HYPER formulation recovers each true pulse amplitude by subtracting the intervening tails of the preceding pulses.

Tail subtraction has also been examined in different other forms. It is possible to reconstruct the overlapped parts of a signal by extrapolation, to be subtracted from the original waveform [8,13–17]. This requires appropriate modelling of the detector pulse, at least the piece of data available between the peak point of the preceding pulse and the start point of the pile-up pulse. By this approach, we are able to recover not only the pulse amplitude, but also its shape and temporal characteristics.

The trailing edges of the amplifier or preamplifier output pulses are governed by the time constants of some RC circuits [1,6,7]. It usually inspires using single- or multiple-term exponential models for fitting [8, 14,17,18]. Even a mono-exponential model like Eq. (1) (as the simplest case) is nonlinear. So for model parameter estimation, the nonlinear least squares (NLS) algorithm is usually used. NLS algorithm can become unacceptably time-consuming due to its iterative nature, noisy or sparse nature of the data and badly-assigned initial values or stopping criteria of the algorithm.

The idea of the current study is to examine simple non-iterative solutions for pulse tail extrapolation, as part of a pile-up correction procedure, in order to reduce the computation time while maintaining the precision of the results. A method of exponential fitting is examined which uses the first-order integral of the pulse data. A linear fitting strategy, as an even more simplified approach is also studied.

2. Materials and methods

In the following, first the setup for experimental data acquisition is described. Then the processing algorithms and the pile-up identification method are explained in details.

2.1. Experimental setup

Experimental data of the present work are acquired by a SCIONIX HOLLAND NaI(Tl) scintillation detector (type 51B51/2M, with both crystal diameter and thickness of 2"), placed in front of a ~49 mCi ^{137}Cs radioactive source (see Fig. 1).

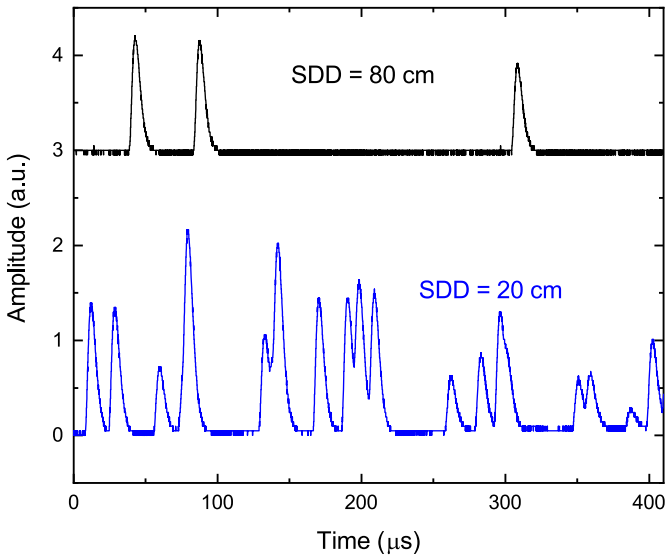

Fig. 2. Pieces of the waveforms obtained by setting SDD equal to 80 and 20 cm.

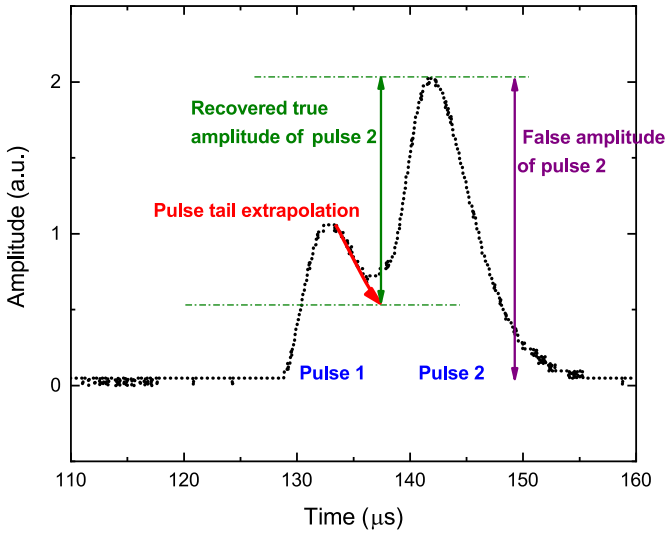

Fig. 3. Schematic representation of the pile-up correction method, in which the data between the peak point of pulse 1 and the start point of pulse 2 are used for extrapolating the tail of pulse 1. The extrapolated tail provides a reference point at the start point of pulse 2, with respect to which the true amplitude of pulse 2 is recovered.

To prevent from very high fluxes of radiation on detector, the detector entrance window is enclosed by a jacket-type single-hole lead collimator. NaI(Tl) crystal is coupled to a photomultiplier tube (PMT). The PMT output pulses are read out by a charge-sensitive preamplifier, then shaped by an amplifier. The amplifier, as well as the bias supplies for the detector (the high voltage, HV) and the preamplifier are provided by a Novin Teyf NT-124 (HVMCA) device. The amplifier output pulses are then fed to an InstruStar-ISDS205A card, functioning as a USB data recorder by which analog data are digitized by a rate 24 MHz. Digitized data are finally saved and analyzed on an Acer Aspire E1-571G laptop (Core i5, 2.6 GHz with 4 GB DDR3 memory).

Two different source-detector distances (SDDs) 80 and 20 cm are considered, called SDD80 and SDD20 hereafter, in order to have both cases of low and high count rate. Each dataset is acquired in a ~1 s time. Parts of the recorded waveforms of these two cases are provided in Fig. 2. Double and triple pile-up events are obvious in the case of SDD20. Pulse width is approximately 15 μs.

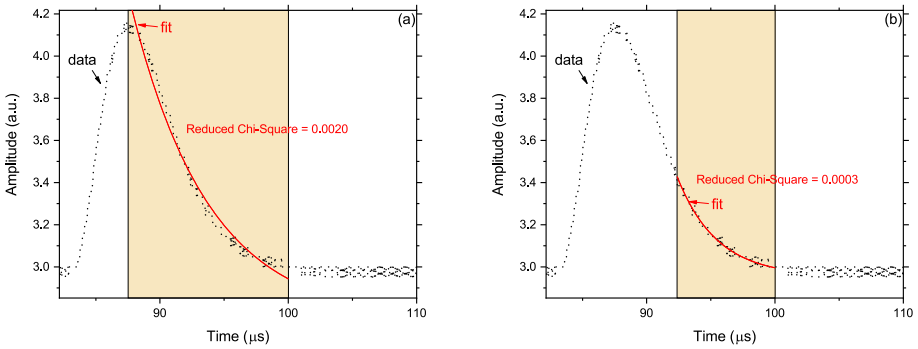

Fig. 4. Fitting a pileup-free experimental pulse by a mono-exponential model by taking into account a) all data and b) the second half of the data on the pulse trailing edge. The latter case has provided better results.

2.2. Processing strategies and algorithms

The present study focuses on pulse tail extrapolation technique, in which the undistorted data between the peak point of a pulse and the start point of the next pulse is used for reconstructing the overlapped part of the first pulse. This way the extrapolated tail provides a corrected reference for calculating the true amplitude of the next pulse, which was affected by pulse pile-up (see Fig. 3). This strategy has been studied in previous works [19–21].

This method, despite its simplicity, is applicable only with appropriate models for pulse fitting. Pulse shape, in general is governed by the detector itself and the time constants of the associated electronics. However, the time characteristics of the detector are more reflected in the pulse rising edge, which are of minimum importance for "tail" extrapolation. If pulses are taken from the preamplifier, which can be modeled by an equivalent RC circuit, the decay of the pulse trailing edge is mainly governed by $\tau = RC$. However, this time constant is usually chosen much larger than the charge collection time of the detector and therefore, in conventional systems the pulses are shaped by a subsequent shaper module [1].

A properly-designed shaper can efficiently reduce the pile-up probability, however, if the event rate becomes very high, the amplitudes of the shaper output pulses may not be preserved and therefore, the energy resolution of the system starts to degrade. This is where the pile-up correction procedures come into play.

Depending on the point where the pulses are taken from (directly from the detector, from the preamplifier or from the shaper), different simple to complicated pulse models have been proposed in the literature [18,22]. When dealing with the pulses of preamplifier or shaper, sums of i exponential terms like Eq. (2) are suitable for modelling the pulse trailing edge, as it is governed by resistive-capacitive circuits which regulate the retreat of the pulse to its baseline by their time constants.

$$V[n] = \sum_{i} A_i e^{-\alpha_i n} \ (i = 1, 2, 3, \ldots) \tag{2}$$

Exponential terms, however, are non-linear, which necessitates the use of appropriate methods for fitting, usually the non-linear least squares (NLS). In least squares approach, the idea is to minimize an objective function of the sum of the squares of the errors between a parametric model and a set of experimental datapoints. If the model is linear, the least squares objective would be quadratic, able to be minimized in one step via a solution to a system of linear equations [23]. For non-linear problems, there is an iterative procedure, needing appropriate initial solutions and stopping criteria, with a possibility of getting stuck in local minima or maxima of the solution space.

In the current study we aim to simplify the solution to the problem. Therefore, a mono-exponential pulse model is selected by setting $i = 1$ in Eq. (2), which results in Eq. (1). This is, however, still a non-linear model. For fitting exponential models to radiation detector pulses, there have been proposed fast, non-iterative alternatives to NLS which work based on integration(s) of the original data [8,9,20,24]. For this solution, let us start from the first-order integral of Eq. (1), $V^{(1)}[n]$ as follows [25]:

$$V^{(1)}[n] = \sum_{k=n}^{N} V[k] \tag{3}$$

Consider an integral equation as a weighted sum of Eqs. (1) and (3) as follows [20]:

$$V[n] + \alpha_1 V^{(1)}[n] - A_1 = 0 \tag{4}$$

Based on Eq. (4), a system of linear equations can be established:

$$\begin{bmatrix} -V^{(1)}[1] & 1 \\ -V^{(1)}[2] & 1 \\ \vdots & \vdots \\ -V^{(1)}[N] & 1 \end{bmatrix} \begin{bmatrix} \alpha_1 \\ A_1 \end{bmatrix} = \begin{bmatrix} V[1] \\ V[2] \\ \vdots \\ V[N] \end{bmatrix} \tag{5}$$

Having known $V[n]$ and $V^{(1)}[n]$, the above system can be solved to finally obtain A_1 and α_1 as the unknown parameters of the mono-exponential model. This solution is free of the need for iterative procedures with answers sufficiently robust against noise (due to the integration embedded in the proposed formulation).

A careful inspection of the experimental pulses reveals that the mono-exponential model might not sufficiently represent the long pulse tails. An example is shown in Fig. 4a. Fitting can be improved by using more than one exponential terms, as in Eq. (2). Similar integral-equation based solutions can be derived for such cases [24–26], however, these mathematical models are obviously more complicated with more parameters to be estimated.

To conserve the idea of using a simple mono-exponential model, we can decide not to fit all the available datapoints on the pulse trailing edge. This comes from the fact that if a signal is composed of several exponential terms of different α_i values, terms of larger α_i will decay faster so that their effect becomes ignorable once an appropriate amount of time is passed. Therefore, a simpler exponential model is more prone to fit the final parts of the signal. In this study, both the cases of using "all the available datapoints" of the pulse trailing edge (similar to Fig. 4a), and the case of using "only the second half of the available data" of the trailing edge (shown in Fig. 4b) are examined.

It should be remarked that the pulse on Fig. 4 has all its data available with no pile-up effect. For pile-up cases, the data on trailing edge becomes limited by the arrival of the next pulse.

To further simplify the solution, the mono-exponential model can be replaced by a linear model as follows:

$$V[n] = Bn + C \tag{6}$$

where B and C are the slope and intercept of the linear model to be estimated. This is in fact the idea of linear approximation of continuous

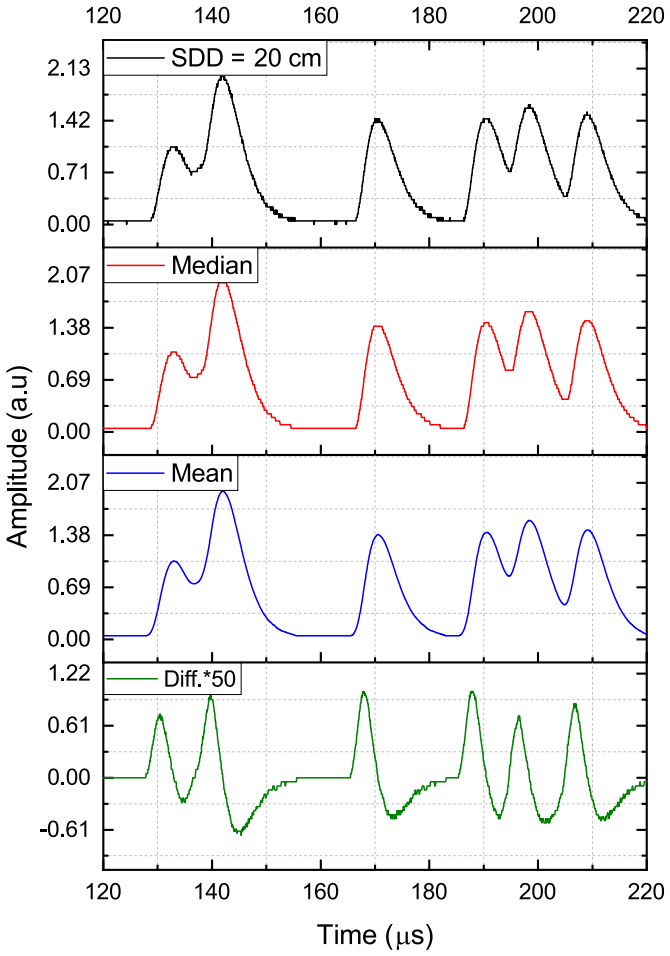

Fig. 5. A leading edge detection strategy for determining the pulse arrival times. From top to bottom: the original waveform (here, part of the SDD20 waveform) is smoothed by the application of a moving median filter, then a moving mean filter (both with window size = 50). Then the first derivative of the smoothed waveform is taken (shown on bottom, arbitrarily multiplied by 50). A threshold on the derivative signal determines the arrival times of the pulses.

functions in sufficiently short pieces of their domain. This can be relevant in detection systems of very high event rate, in which the pulses arrive very close to each other. Another case is when the pulses are taken from the preamplifier, with very long tails which are well approximated by a linear behavior [21]. For this approach, a system of linear equations can be established and solved for B and C according to Eq. (6) [21]:

$$\begin{bmatrix} 1 & 1 \\ 2 & 1 \\ \vdots & \vdots \\ N & 1 \end{bmatrix} \begin{bmatrix} B \\ C \end{bmatrix} = \begin{bmatrix} V[1] \\ V[2] \\ \vdots \\ V[N] \end{bmatrix} \tag{7}$$

2.3. Pile-up identification method

Experimental data of the present study reveal a pulse length of approximately 15 μs. Therefore, pulses with arrival times closer than 15 μs are considered as pile-up cases. To identify these cases, the pulse arrival times were determined and compared by a leading edge detection method. See Fig. 5 for the procedure in which, first the recorded waveform was smoothed by a successive application of a moving median and a moving mean filter, both with a fixed window size of 50 samples. Then the first derivative of the smoothed waveform was taken and compared with an appropriate threshold level. This way the arrival

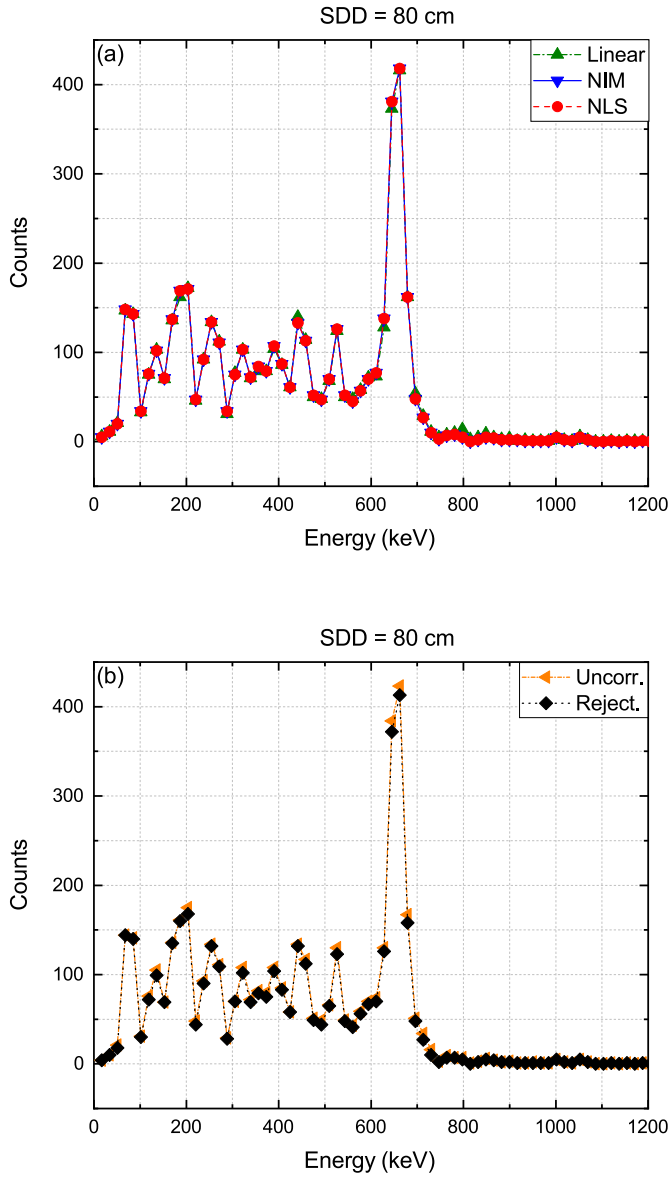

Fig. 6. Energy spectra calculated for the SDD80 dataset by strategy 1. (a): Pileup-corrected spectra by mono-exponential fitting by the non-iterative method (NIM), linear fitting and mono-exponential fitting by non-linear least squares (NLS) method. (b): The uncorrected spectrum, as well as the pileup-rejected spectrum for the same dataset.

times of all pulses were obtained, based on which the time intervals between the successive pulses were determined. A comparison between the calculated time intervals with the typical pulse length 15 μs helped finding the pile-up cases.

The piled-up pulses were first processed by the tail extrapolation algorithms discussed in section 2.2, then their recovered amplitudes determined. The amplitudes of the pileup-free pulses were recorded directly. Finally all the calculated pulse amplitudes were used to fill the channels of the pulse height distribution.

3. Results and discussion

Results of the analysis of the two experimental datasets obtained by placing the detector at SDDs 80 and 20 cm (see section 2.1) are presented in the following. Each dataset was inspected by the leading edge detection method described in section 2.3 to find the piled-up pulses. The amplitudes of the pileup-free pulses were recorded first. Then the

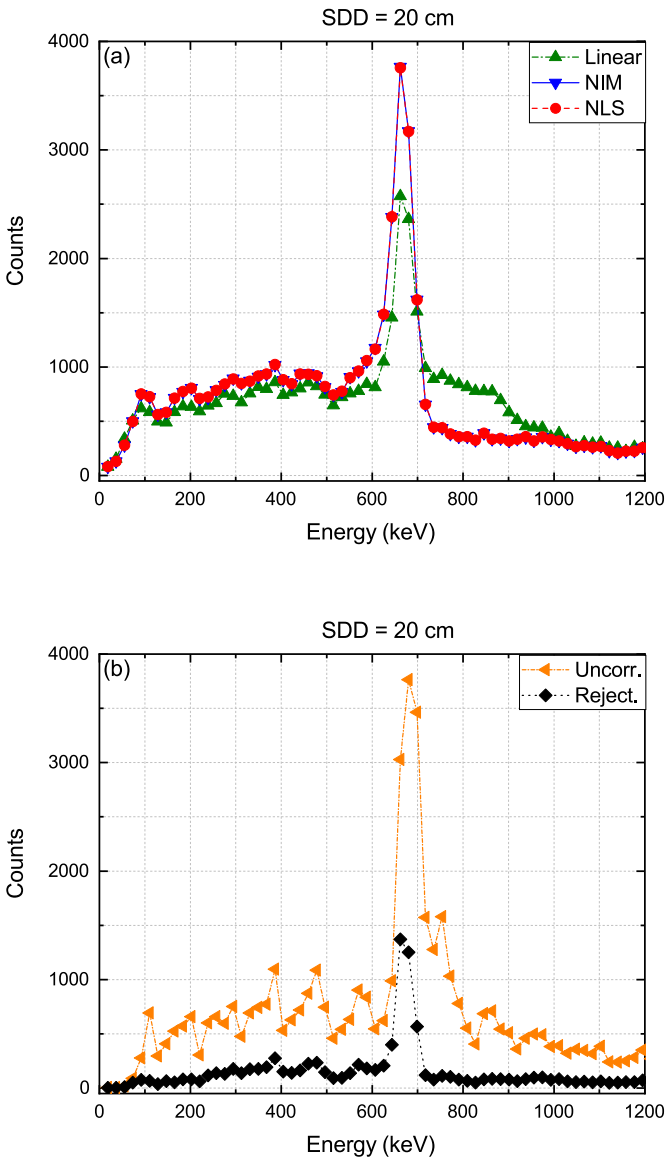

Fig. 7. Energy spectra calculated for the SDD20 dataset by strategy 1. (a): Pileup-corrected spectra by NIM, linear fitting and NLS methods. (b): The uncorrected spectrum, as well as the pileup-rejected spectrum for the same dataset.

pile-up cases were processed by the non-iterative method of Eq. (5), the linear approximation of Eq. (7), and the NLS method. The latter case uses the "fit" function of MATLAB R2016b with a single-term exponential function and all other fit options set to MATLAB defaults. Both systems of linear equations of Eqs. (5) and (7) were solved by the matrix left division operator of MATLAB, which provides a least squares solution due to the fact that the coefficient matrices of both Eqs. (5) and (7) are non-square.

All calculations were repeated twice:

- By tail extrapolation using only the second half of the available (undistorted) data on the pulse trailing edge. This is similar to the case of Fig. 4b, called "strategy 1" hereafter.
- By considering all the available data of each pulse. This is similar to the case of Fig. 4a, called "strategy 2" hereafter.

Complex, negative, infinity or undefined values in fitting results were discarded in spectrum calculations.

Table 1
FWHM values in keV for the energy spectra of Figs. 6 and 7. FWHMs are calculated around the full-energy peak of each spectrum.

	SDD	
Method	80 cm (from Fig. 6)	20 cm (from Fig. 7)
NIM	42.8	62.3
NLS	42.8	62.4
Linear	42.3	70.7
Rejection	42.1	46.6
Uncorrected[a]	42.5	62.5

[a] Note the shift in peak position of the uncorrected spectrum for SDD20 dataset.

3.1. Calculating the energy spectra by strategy 1

In strategy 1, pile-up correction is accomplished by extrapolating the pulse tails by using the second half of the available data of each pulse. Fig. 6a shows for SDD80 the spectra calculated by the proposed non-iterative method as well as the NLS and the linear approximation methods. The abscissa of the pulse height distributions are calibrated to represent the energy spectra. For ^{137}Cs, a full-energy peak at 662 keV is expected, with a Compton continuum standing behind. Compton continua of Fig. 6 suffer from relatively large fluctuations due to the poor statistics of the number of pulses recorded in the 1-s acquisition time (see section 2.1). Results for all the three NIM, NLS and linear methods are almost the same, as expected, because the pile-up cases for SDD80 are rare with no observable effect on the energy spectra. This is better understood by comparing Fig. 6a with Fig. 6b, in which the uncorrected spectrum, as well as the pileup-rejected spectrum are calculated for the same dataset. The uncorrected spectrum is obtained by the amplitudes of all pulses in the original waveform, with no correction method applied. In pile-up rejection approach, all pileup-distorted pulses are discarded. The uncorrected and the pile-up rejection spectra are not too different from each other and from the spectra of Fig. 6a, which confirms the minor effect of the very small number of pile-up cases for SDD80 dataset.

Fig. 7 illustrates the analysis results for the case of SDD20, with a procedure similar to the case of SDD80 explained above. The SDD20 dataset contains considerable pile-up cases. This could be observed by looking at the piece of the SDD20 dataset on Fig. 2, or by comparing the area under the uncorrected spectrum and the pile-up rejection spectrum on Fig. 7b.

Due to pile-up effects, the full-energy peak of the uncorrected spectrum in Fig. 7b is slightly shifted to a higher energy channel. Fig. 7a illustrates the corrected spectra, in which all the three NIM, NLS and linear extrapolation methods have recovered the full-energy peak back to its expected energy channel at 662 keV. The corrected spectra of NIM and NLS are very similar in all features. The full-energy peak by linear extrapolation is, however, of a lower level in comparison with NIM and NLS. This is due to the inconsistency of the linear approximation, which can result in unacceptable fitting outputs (complex numbers, negative values, etc.) that are discarded; or due to the incorrect fitting outputs taken into account (for example, see on Fig. 7a the plateau and plain patterns for the linear extrapolation spectrum between 700 and 1000 keV).

It should be remarked that Compton valleys in spectra of Fig. 7a are so filled that it is difficult to detect a clear Compton edge on the spectra. This can be attributed to the large number of multiple Compton scattering events in the detector, as well as the Compton events scattered from the collimator into the detector.

More details of the analysis of both datasets SDD20 and SDD80 are provided in the following. The values of full width at half maximum (FWHM), as a measure of energy resolution are provided in Table 1. For the case of SDD80, FWHMs are almost the same, due to the fact that the pile-up cases are very rare, with minimum effect on the shape of the spectrum. For the case of SDD20, the best energy resolution is obtained

Table 2
The number of full-energy counts (the area under peak from 600 to 724 keV) to the total number of counts (the area under the curve from 0 to 1200 keV) for the energy spectra of Figs. 6 and 7.

	SDD	
Method	80 cm (from Fig. 6)	20 cm (from Fig. 7)
NIM	21417/72284	257359/856194
NLS	21417/72284	257065/856742
Linear	21158/72326	193514/825065
Rejection	20785/69763	74333/181168
Uncorrected	21638/72394	252138/842909

Table 3
MATLAB computation times (in seconds) for processing the pile-up cases of SDD = 80 and 20 cm datasets by NIM, NLS and linear extrapolation methods based on strategy 1. Results are the mean values for three times repetition of each measurement.

	SDD	
Method	80 cm	20 cm
NIM	1.00 ± 0.05	17.95 ± 0.15
NLS	4.30 ± 0.25	1020.10 ± 12.00
Linear	0.005 ± 0	0.65 ± 0.05

for the pile-up rejection spectra, at the expense of a considerable drop in the number of accepted pulses (see Table 2). Table 1 also shows the poorest FWHM for the spectrum of linear extrapolation, mainly due to the failure of the linear model in fitting the pulses of this study.

Table 2 presents for all spectra of Figs. 6 and 7 the total number of full-energy counts to the total number of accepted counts for spectrum calculation in each case, obtained by calculating the area under the spectra respectively from 600 to 724 keV and from 0 to 1200 keV. For the case of SDD80, results are almost similar except for the rejection spectra, where a slightly less number of counts are recorded. The differences become more pronounced in the case of SDD20, where pile-ups become more prominent, and NIM and NLS perform much better than the pile-up rejection and linear extrapolation approaches in preserving the full-energy events and generally, the throughput rate of the system.

Table 3 provides the computation times calculated by the MATLAB "tic" and "toc" functions for the pile-up correction algorithms. Each case was repeated three times to calculate a mean time value. Processing times for the SDD20 dataset are much longer than for SDD80, due to the increase in the number of pile-up cases. Linear extrapolation is the fastest algorithm, due to its reduced complexity. The difference between the computation times of NIM and NLS is quite notable so that NIM is nearly 57 (≈1020.10/17.95) times faster than NLS for the SDD20 dataset, with a similar energy resolution and throughput rate according to Tables 1 and 2. The complexity of NIM is also reduced considerably to be more congruent with hardware implementation on digital signal processing (DSP) boards or field programmable gate arrays (FPGAs).

3.2. Calculating the energy spectra by strategy 2

Analyses of the previous section were based on strategy 1, in which only the second half of the available data on the trailing edge of each pulse were used for tail extrapolation. The piece of data for fitting must be chosen carefully, as it can greatly affect the results. In this section, the strategy 2 is considered, in which all the available data on the pulse trailing edge are used for extrapolation. All other details of the procedure of pulse arrival time determination, pile-up detection and correction by NIM, NLS and linear extrapolation are the same as for strategy 1. Fig. 8a and b illustrate the pileup-corrected spectra by strategy 2 for SDD80 and SDD20 datasets, respectively.

In Fig. 8, the results for SDD80 dataset are very similar to those by strategy 1 shown in Fig. 6a. However, the results for SDD20 dataset have

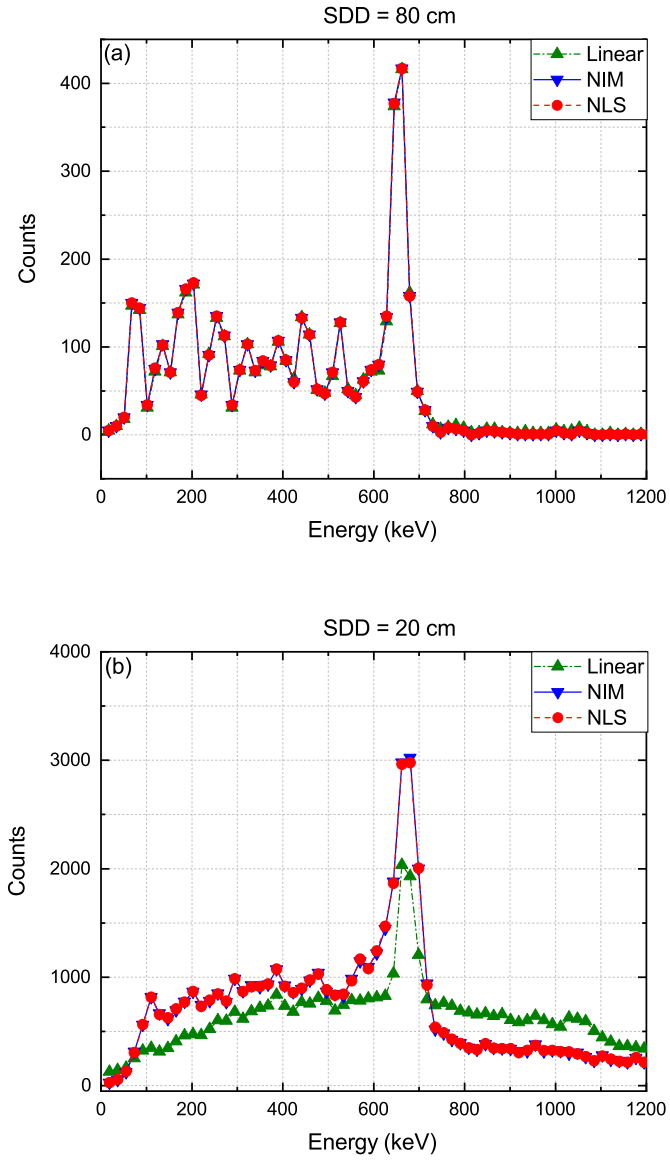

Fig. 8. Energy spectra calculated for the dataset of (a) SDD = 80 cm and (b) SDD = 20 cm by strategy 2. Pileup-corrected spectra by NIM, NLS and linear fitting are illustrated. The uncorrected and the pileup-rejected spectra for cases (a) and (b) are shown in Fig. 6b and 7b, respectively.

Table 4
FWHM values in keV for the energy spectra of Fig. 8

	SDD	
Method	80 cm (from Fig. 8a)	20 cm (from Fig. 8b)
NIM	42.4	79.3
NLS	42.4	81.5
Linear	42.4	65.1

degraded substantially: the heights of the full-energy peaks of NIM and NLS in Fig. 8b are about 0.8 (≈3000/3760) of those of Fig. 7a. This is also the case for the linear extrapolation results (2040/2570 ≈ 0.8). This is due to the failure in recovering true amplitudes of some full-energy pulses, which are misregistered in channels adjacent to the expected channel on the energy spectrum. This can broaden the full-energy peak. A comparison between the FWHMs of the pileup-corrected energy spectra of Fig. 8 reported in Table 4, with the FWHMs in Table 1 shows a nearly 27% ($\approx \frac{79.3-62.3}{62.3}$) increase in FWHM for the NIM spectra of

Table 5
The number of full-energy counts (the area under peak from 600 to 724 keV) to the total number of counts (the area under the curve from 0 to 1200 keV) for the energy spectra of Fig. 8

	SDD	
Method	80 cm (from Fig. 8a)	20 cm (from Fig. 8b)
NIM	21309/72301	242386/858155
NLS	21309/72301	241520/858407
Linear	21096/72233	155059/766671

Table 6
Mean MATLAB computation times (in seconds) for processing the pile-up cases of SDD = 80 and 20 cm datasets by NIM, NLS and linear extrapolation methods based on strategy 2.

	SDD	
Method	80 cm	20 cm
NIM	3.50 ± 0.05	43.05 ± 0.10
NLS	4.85 ± 0.35	1195.95 ± 1.90
Linear	0.005 ± 0	0.75 ± 0

SDD20. This is more or less the case also for NLS.

FWHMs of the spectra by strategy 1 and strategy 2 are almost the same for the SDD80 dataset. This is also true for the calculated number of full-energy events: compare in this regard the results by strategy 2 (on Table 5) with those by strategy 1 (on Table 2). Nevertheless, results are quite different for the case of SDD20, where strategy 2 shows reduced numbers of full-energy events for all pile-up correction methods.

The computation times for calculating the energy spectra by strategy 2 were also obtained. Results are presented in Table 6, which show an overall increase in computation time in comparison with strategy 1 (see Table 3). It can be attributed to the increased number of data-points in strategy 2 which results in larger matrix formulations of the problem. Moreover, the insufficiency of the parametric model can increase the computation time of the least squares method to reach a mathematically acceptable result. The NIM computation time has experienced the most increase both for SDD80 and SDD20 datasets, however, it requires an absolute time still much less than the time required by the NLS method.

4. Conclusions

Concentrated on the problem of pulse pile-up correction in radiation detection systems, this article examined two non-iterative approaches for pulse tail extrapolation: an integral-equation based method for mono-exponential fitting, and a linear fitting method. The integral-equation based approach was shown to perform similar with the non-linear least squares method with considerably improved speed (nearly 57 times faster for a high count rate dataset in the present study) and reduced complexity of the algorithm. Linear fitting showed the fastest performance, however with a degradation of energy resolution and throughput rate at high count rates, due to the insufficiency of the linear model for pulse fitting. The necessity to choose an appropriate piece of data for fitting was also discussed by considering two scenarios of fitting "all" or "the second half" of the available data of each pulse.

In sum, the proposed integral-equation based method was proven to be a simple, fast, non-iterative alternative to the conventional non-linear least squares method, in order to simplify and speed up the processing schemes especially for hardware implementation on DSPs and FPGAs.

Declaration of competing interest

The authors declare that they have no known competing financial interests or personal relationships that could have appeared to influence the work reported in this paper.

Acknowledgements

The author appreciates the technical support by Fatemeh Nowrouz-Alizadeh and Mosayeb Dehghani, the scientific staffs of the Shiraz University laboratories at the Radiation Research Center (RRC) and the Department of Mechanical Engineering, respectively.

References

[1] G.F. Knoll, Radiation Detection and Measurement, fourth ed., John Wiley & Sons, 2010.
[2] N. Tsoulfanidis, Measurement and Detection of Radiation, fourth ed., CRC Press, 2015.
[3] S.N. Ahmed, Physics and Engineering of Radiation Detection, second ed., Elsevier, 2014.
[4] L. Abbene, et al., Recent advances in the development of high-resolution 3D cadmium–zinc–telluride drift strip detectors, J. Synchrotron Radiat. 27 (6) (2020) 1564–1576.
[5] L. Abbene, et al., Potentialities of high-resolution 3-D CZT drift strip detectors for prompt gamma-ray measurements in BNCT, Sensors 22 (4) (2022) 1502.
[6] P.W. Nicholson, Nuclear Electronics, John Wiley and Sons, Inc., London, 1974.
[7] M. Nakhostin, Signal Processing for Radiation Detectors, John Wiley & Sons, 2017.
[8] M.-R. Mohammadian-Behbahani, S. Saramad, Pile-up correction algorithm based on successive integration for high count rate medical imaging and radiation spectroscopy, Nucl. Instrum. Methods Phys. Res. Sect. A Accel. Spectrom. Detect. Assoc. Equip. 897 (2018) 1–7.
[9] M.-R. Mohammadian-Behbahani, S. Saramad, A comparison study of the pile-up correction algorithms, Nucl. Instrum. Methods Phys. Res. Sect. A Accel. Spectrom. Detect. Assoc. Equip. 951 (2020), 163013.
[10] X. Wen, H. Yang, Study on a digital pulse processing algorithm based on template-matching for high-throughput spectroscopy, Nucl. Instrum. Methods Phys. Res. Sect. A Accel. Spectrom. Detect. Assoc. Equip. 784 (2015) 269–273.
[11] B. Löher, D. Savran, E. Fiori, M. Miklavec, N. Pietralla, M. Vencelj, High count rate γ-ray spectroscopy with LaBr3: Ce scintillation detectors, Nucl. Instrum. Methods Phys. Res. Sect. A Accel. Spectrom. Detect. Assoc. Equip. 686 (2012) 1–6.
[12] J. Liu, et al., Real time digital implementation of the high-yield-pileup-event-recover (HYPER) method, in: Nuclear Science Symposium Conference Record, vol. 6, 2007, pp. 4230–4232.
[13] S. Marrone, et al., Pulse shape analysis of liquid scintillators for neutron studies, Nucl. Instrum. Methods Phys. Res. Sect. A Accel. Spectrom. Detect. Assoc. Equip. 490 (1–2) (Sep. 2002) 299–307.
[14] W. Guo, R.P. Gardner, C.W. Mayo, A study of the real-time deconvolution of digitized waveforms with pulse pile up for digital radiation spectroscopy, Nucl. Instrum. Methods Phys. Res. Sect. A Accel. Spectrom. Detect. Assoc. Equip. 544 (3) (2005) 668–678.
[15] F. Belli, B. Esposito, D. Marocco, M. Riva, Y. Kaschuck, G. Bonheure, A method for digital processing of pile-up events in organic scintillators, Nucl. Instrum. Methods Phys. Res. Sect. A Accel. Spectrom. Detect. Assoc. Equip. 595 (2) (2008) 512–519.
[16] X. Wang, Q. Xie, Y. Chen, M. Niu, P. Xiao, Advantages of digitally sampling scintillation pulses in pileup processing in PET, IEEE Trans. Nucl. Sci. 59 (3) (2012) 498–506.
[17] M.E. Hammad, et al., Pile-up correction algorithm for high count rate gamma ray spectroscopy, Appl. Radiat. Isot. 151 (2019) 196–206.
[18] J. Pechousek, et al., Software emulator of nuclear pulse generation with different pulse shapes and pile-up, Nucl. Instrum. Methods Phys. Res. Sect. A Accel. Spectrom. Detect. Assoc. Equip. 828 (2016) 81–85.
[19] M. Lee, et al., Pulse pileup correction method for gamma-ray spectroscopy in high radiation fields, Nucl. Eng. Technol. 52 (5) (2020) 1029–1035.
[20] M.R. Mohammadian-Behbahani, A pulse pile-up correction method for high-rate radiation spectroscopy, in: *1st* International & 28th National Conference on Nuclear Science and Technology, 2022. ICNST22.
[21] M.R. Mohammadian-Behbahani, Pulse pile-up correction: a comparison between pulse-tail linear extrapolation and trapezoidal pulse shaping, in: *1st* International & 28th National Conference on Nuclear Science and Technology, 2022. ICNST22.
[22] W. Xiao, A.T. Farsoni, H. Yang, D.H. Hamby, A new pulse model for NaI (Tl) detection systems, Nucl. Instrum. Methods Phys. Res. Sect. A Accel. Spectrom. Detect. Assoc. Equip. 763 (2014) 170–173.
[23] H.P. Gavin, The Levenberg-Marquardt algorithm for nonlinear least squares curve-fitting problems, Dep. Civ. Environ. Eng. Duke Univ. 19 (2019).
[24] M.-R. Mohammadian-Behbahani, S. Saramad, Integral-equation based methods for parameter estimation in output pulses of radiation detectors: application in nuclear medicine and spectroscopy, Nucl. Instrum. Methods Phys. Res. Sect. A Accel. Spectrom. Detect. Assoc. Equip. 887 (2018) 7–12.
[25] K. Tittelbach-Helmrich, An integration method for the analysis of multiexponential transient signals, Meas. Sci. Technol. 4 (12) (1993) 1323.
[26] S.D. Foss, A Method of Exponential Curve Fitting by Numerical Integration, Biometrics, 1970, p. 815. –821.